Tribology Letters, Vol. 18, No. 1, January 2005 (© 2005)
DOI: 10.1007/s11249-004-1758-7

Effects of lubricant additives on the performance of hydrodynamically lubricated journal bearings

A.A. Elsharkawy*

Department of Mechanical Engineering, College of Engineering and Petroleum, Kuwait University, P.O. Box 5969, Safat 13060, Kuwait

Received 20 February 2004; accepted 21 May 2004

A non-Newtonian rheological model to investigate theoretically the effects of lubricant additives on the steady state performance of hydrodynamically lubricated finite journal bearings is introduced. In this model, the non-Newtonian behavior resulting from blending the lubricant with polymer additives is simulated by Stokes couple stress fluid model. The formed boundary layer at the bearing surface is described through the use of a hypothetical porous medium layer that adheres to the bearing surface. The Brinkman-extended Darcy equations are utilized to model the flow in the porous region. A stress jump boundary condition is applied at the porous media/fluid film interface. A modified form of the Reynolds equation is derived and solved numerically using a finite difference scheme. The effects of bearing geometry, and non-Newtonian behavior of the lubricant on the steady-state performance characteristics such as pressure distribution, load carrying capacity, side leakage flow, and coefficient of friction are presented and discussed. The results showed that lubricant additives significantly increase the load carrying capacity and reduce both the coefficient of friction and the side leakage as compared to the Newtonian lubricants.

KEY WORDS: journal bearings, non-Newtonian fluids, lubricant additives, hydrodynamic lubrication, porous media

Nomenclature

c	radial clearance, m
C_0	flexibility parameter
e	eccentricity, m
E	modulus of elasticity of the bearing liner, Pa
f	friction coefficient
h	film thickness, m
H	dimensionless film thickness, $H = h/c$
k	permeability of bearing material, m^2
K	dimensionless permeability, $K = k/c^2$
L	length of the bearing, m
$\bar{\ell}$	couple stress parameter, $\bar{\ell} = (\eta/\mu)^{1/2}/c$
p	pressure of lubricant film, Pa
$p*$	pressure of the lubricant within the porous layer, Pa
p_s	supply pressure of lubricant film, Pa
P	dimensionless pressure, $P = pc^2/\mu UR$
P_s	dimensionless supply pressure of lubricant film, $P_s = p_s c^2/\mu UR$
q_s	side leakage flow, m^3/s
Q_s	dimensionless side leakage flow, $Q_s = q_s/URc$
R	radius of the journal, m
t_ℓ	thickness of the bearing liner, m
u	velocity of the lubricant film in x-direction, m/s
$\bar{u}$	dimensionless velocity of the lubricant film in x-direction, $\bar{u} = u/U$
u^*	local mean (ensemble-averaged) velocity of the lubricant within the porous matrix in x-direction, m/s
$\bar{u}^*$	dimensionless local mean (ensemble-averaged) velocity of the lubricant within the porous matrix in x-direction, $\bar{u}^* = u^*/U$
U	surface velocity of the journal, $U = \omega R$, m/s
v	velocity of the lubricant film in y-direction.
w	velocity of the lubricant film in z-direction.
$\bar{w}$	dimensionless velocity of the lubricant film in z-direction, $\bar{w} = w/U$
w^*	local mean (ensemble-averaged) velocity of the lubricant within the porous matrix in z-direction, m/s
$\bar{w}^*$	dimensionless local mean (ensemble-averaged) velocity of the lubricant within the porous matrix in z-direction, $\bar{w}^* = w^*/U$
w_{load}	total load capacity of the bearing, N
W	dimensionless load capacity of the bearing, $W = w_{load}c^2/(\mu UR^2L)$
x, y, z	bearing coordinates in circumferential, radial, and axial directions, respectively
X, Y, Z	dimensionless coordinates in circumferential, radial, and axial directions, respectively, $X = x/R$, $Y = y/c$, $Z = z/L$.
α	dimensionless parameter, $\alpha = (\mu^*/\mu)^{1/2}$
β	stress jump parameter
δ	thickness of the porous layer, m
Δ	dimensionless thickness of the porous layer, $\Delta = \delta/c$
ε	eccentricity ratio, e/c
θ	angular coordinate, rad
μ	viscosity of the lubricant in the film region, Pa s
$\mu*$	effective viscosity of the lubricant in the porous matrix, Pa s
ν	Poisson's ratio of the porous liner material
ρ	lubricant density, kg m^3
Φ	attitude angle (see figure 1), rad
ω	angular velocity of the journal, rad/s

*E-mail: abdallah@kuco1.kuniv.edu.kw

1. Introduction

Journal bearings are used extensively in rotating machines because of their low wear and good damping characteristics. Typical applications include turbines, large milling systems, engine cranks, compressors, gearboxes, etc. In these bearings, a hydrodynamic film occurs when there is sufficient lubricant between the lubricated surfaces at the point of loading to form a fluid wedge that separates the sliding surfaces. Recent experimental studies showed that the performance of

lubricated contacts could be improved by blending the base oil with additives. These additives can thicken the lubricant film thickness and form a solid thin boundary layer that adheres to the lubricated surfaces. This thin layer protects the surfaces from degradation and reduces the frictional force. Oliver [1] showed experimentally that additive of dissolved polymer in the lubricant improves the load carrying capacity and reduces the friction coefficient in short journal bearings. Spikes [2] examined base oil blended with some additives to balance the behavior of the lubricant in elastohydrodynamically lubricated contacts and consequently reduce friction and surface damage. Furthermore, Durack *et al*. [3] observed a substantial reduction of friction in engine journal bearings when oil fortifier (oil additives) was added to the base oil. The present study is an attempt to introduce a theoretical approach using a non-Newtonian fluid model which describes the experimentally observed features of the lubricant within the conjunction to investigate the effects of the lubricant additives on the steady state performance of hydrodynamically lubricated finite journal bearings.

Non-Newtonian behavior is generally a function of the structural complexity of fluids. Lubricants containing additives should be treated as non-Newtonian fluids. In the literature, two models are widely used to describe the non-Newtonian behavior of the lubricant in hydrodynamically lubricated conformal conjunctions. The first rheological model is the well-known power-law fluid model [4,5]. The second model consists of the couple stress fluid model based on microcontinuum theory derived by Stokes [6]. Stokes' theory is the simplest generalization of the classical theory of fluids, which allows for the polar effects such as the presence of non-symmetric stress tensor, the couple stresses and the body couples. The couple stresses might be expected to appear in noticeable magnitudes in liquids containing additives with large molecules. For this model, the continuity and momentum equations governing the motion of the lubricant in the absence of body forces and body couples are

$$\nabla \cdot V = 0 \tag{1}$$

$$\rho \frac{DV}{Dt} = -\nabla p + \mu \nabla^2 V - \eta \nabla^4 V \tag{2}$$

where V is the velocity vector, ρ is the density, p is the pressure, μ is the classical viscosity coefficient, and η is a material constant for couple stress with the dimensions of momentum. Many investigators have used couple stress theory of fluids to study static and dynamic characteristics of various bearings see for examples [7–9]. These studies have led to the predictions such as larger load carrying capacity, lower coefficient of friction, and delayed time of approach compared with the Newtonian case.

From slow squeezing of a thin film between two crossed molecularly smooth mica cylinders, Chan and Horn [10] found that the squeeze rate can be predicted by the classical Reynolds equation down to about 30 nm. They obtained good correlation between theory and experiment by simply adding a fictitious rigid layer of 0.7 nm to the mica surface. Based on these experimental observations, Tichy [11] was able to develop a rheological model, which can be applied to boundary lubrication. He considered the fictitious rigid layer considered by Chan and Horn [10] as a solid porous layer adhered to the solid surfaces due to the lubricant microstructure. Darcy law, which says that the local flow velocity relative to the porous medium is proportional to the pressure gradient, and inversely proportional to the viscosity, was used to describe the fluid flow through the porous medium. Li [12] modified Tichy's model by using Brinkman-extended Darcy model, which takes into account the viscous shear effects and the viscous damping effects, to describe the fluid flow in the porous medium. The Brinkman-extended Darcy model is also appropriate for thin porous media with high permeability. A shear stress jump condition was applied at the porous media/fluid film interface. The experimental observations by Nield [13] and the study of Ochoa-Tapia and Witaker [14] supported the idea of inclusion of the stress jump boundary condition at the porous media/fluid film interface.

In the present study, both the porous media model and the couple stress model are utilized to study the effects of lubricant additives on the performance of hydrodynamically lubricated journal bearings. The porous media model was developed by Tichy [11] and modified by Li [12]. Making use of the Brinkman extended-Darcy model with stress jump boundary condition at the porous media/fluid film interface and the couple stress model, a modified form of Reynolds equation is derived. A finite difference scheme is implemented to solve for the pressure distribution within the lubricated conjunction. The effects of bearing geometry, and non-Newtonian behavior of the lubricant on the steady-state performance characteristics such as pressure distribution, load carrying capacity, side leakage flow, and friction factor are presented and discussed.

2. Mathematical model

The coordinate system and the configuration of one-layered journal bearing are shown in figure 1. It is assumed that the journal and bearing are circular, the load is applied in y-direction, the groove is filled with a lubricant of constant pressure, and the journal rotates with a constant angular velocity ω about its

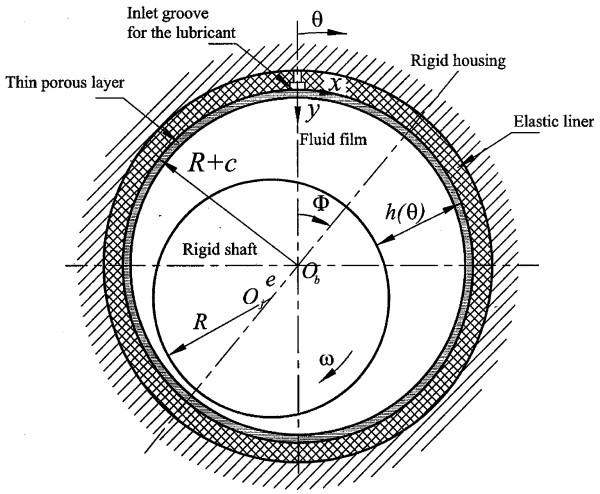

Figure 1. Bearing geometry.

axis. An elastic liner of thickness t_ℓ and elastic properties E, and v is press-fitted in a rigid housing. A porous layer of thickness δ is attached to the stationary bearing surface. The porous film thickness is assumed to be smaller than the thickness of the lubricant. Physically, the thickness of the porous layer represents presumably known molecular scale of the lubricant [11]. In the present analysis the following assumptions are also considered: the porous matrix is homogenous and isotropic, the variation of the pressure across the porous layer and the fluid film is negligible, the inertia effects are negligible, the thermal effects are not considered, and the journal is rigid.

The lubricant flow in the porous region ($0 \le y \le \delta$) is governed by the Brinkman equation [15], which accounts for the viscous shear effects and the viscous damping effects (Darcy resistance)

$$\frac{\partial p^*}{\partial x} = -\frac{\mu}{k}u^* + \mu^*\frac{\partial^2 u^*}{\partial y^2} \tag{3}$$

$$\frac{\partial p^*}{\partial y} = 0 \tag{4}$$

$$\frac{\partial p^*}{\partial z} = -\frac{\mu}{k}w^* + \mu^*\frac{\partial^2 w^*}{\partial y^2} \tag{5}$$

where μ^* and μ are the effective viscosity of the lubricant within the porous layer and the film region, respectively, p^* is the pressure of the lubricant within the porous layer, u^* and w^* are the local mean (ensemble-averaged) velocities in the x and z directions within the porous layer, respectively.

The lubricant flow in the film region ($\delta \le y \le h$) obeys Stokes' couple stress model [6]. Under the usual assumptions of lubrication applicable to thin films, equations (1) and (2) in this case can be written as

$$\frac{\partial u}{\partial x} + \frac{\partial v}{\partial y} + \frac{\partial w}{\partial z} = 0 \tag{6}$$

$$\frac{\partial p}{\partial x} = \mu\frac{\partial^2 u}{\partial y^2} - \eta\frac{\partial^4 u}{\partial y^4} \tag{7}$$

$$\frac{\partial p}{\partial y} = 0 \tag{8}$$

$$\frac{\partial p}{\partial z} = \mu\frac{\partial^2 w}{\partial y^2} - \eta\frac{\partial^4 w}{\partial y^4} \tag{9}$$

where p is the pressure in the film region, u and w are the velocities in the x and z directions within the film region, respectively.

The boundary conditions are that the velocities match at the porous medium/fluid film interface, the couple stress vanishes at the interface, and no-slip boundary conditions at the impermeable surface:

(a) At the rigid housing-porous layer interface ($y = 0$):

$$u^* = w^* = 0 \tag{10}$$

(b) At the porous layer–fluid film interface ($y = \delta$):

$$u^* = u, \quad w^* = w \tag{11}$$

$$\mu^*\frac{\mathrm{d}u^*}{\mathrm{d}y} - \mu\frac{\mathrm{d}u}{\mathrm{d}y} = \beta\frac{\mu}{\sqrt{k}}u^* \tag{12}$$

$$\frac{\partial^2 u}{\partial y^2} = 0, \quad \frac{\partial^2 w}{\partial y^2} = 0 \tag{13}$$

where β is the stress jump parameter.

(c) At the shaft–fluid film interface ($y = \mathrm{h}$)

$$u = U, \quad w = 0 \tag{14}$$

where U is the surface velocity of the journal.

From equations (3)–(9) and boundary conditions (10)–(14), the velocity components can be written in the following dimensionless form:

(a) within the porous layer: $0 \le Y \le \Delta$

$$\bar{u}^* = F_1 \sinh\left(\frac{Y}{\alpha\sqrt{K}}\right)\Big/\sinh\left(\frac{\Delta}{\alpha\sqrt{K}}\right) - \frac{\partial p}{\partial\theta}\left[KC_1(Y) + F_2\sinh\left(\frac{Y}{\alpha\sqrt{K}}\right)\Big/\sinh\left(\frac{\Delta}{\alpha\sqrt{K}}\right)\right] \tag{15}$$

$$\bar{w}^* = -\left(\frac{R}{L}\right)\frac{\partial P}{\partial Z}\left[KC_1(Y) + F_2 \sinh\left(\frac{Y}{\alpha\sqrt{K}}\right)/\sinh\left(\frac{\Delta}{\alpha\sqrt{K}}\right)\right] \tag{16}$$

(b) within the fluid film: $\Delta \le Y \le H$

$$\begin{aligned}\bar{u} = {} & F_1 + \frac{Y-\Delta}{H-\Delta}(1-F_1) \\ & - \frac{\partial P}{\partial \theta}\left\{F_2 - \left(\frac{Y-\Delta}{H-\Delta}\right)F_2 - \frac{1}{2}\left(Y^2-\Delta^2\right)\right. \\ & + \frac{1}{2}(Y-\Delta)(H+\Delta) \\ & \left. - \bar{\ell}^{\,2} + \bar{\ell}^{\,2}\frac{\sinh\left(\frac{H-Y}{\bar{\ell}}\right) + \sinh\left(\frac{Y-\Delta}{\bar{\ell}}\right)}{\sinh\left(\frac{H-\Delta}{\bar{\ell}}\right)}\right\}\end{aligned} \tag{17}$$

$$\begin{aligned}\bar{w} = {} & -\left(\frac{R}{L}\right)\frac{\partial p}{\partial Z} \\ & \left\{F_2 - \left(\frac{Y-\Delta}{H-\Delta}\right)F_2\right. \\ & - \frac{1}{2}\left(Y^2-\Delta^2\right) + \frac{1}{2}(Y-\Delta)(H+\Delta) \\ & \left. - \bar{\ell}^{\,2} + \bar{\ell}^{\,2}\frac{\sinh\left(\frac{H-Y}{\bar{\ell}}\right) + \sinh\left(\frac{Y-\Delta}{\bar{\ell}}\right)}{\sinh\left(\frac{H-\Delta}{\bar{\ell}}\right)}\right\}\end{aligned} \tag{18}$$

where

$$C_1(Y) = 1 - \left[\sinh\left(\frac{Y}{\alpha\sqrt{K}}\right) - \sinh\left(\frac{Y-\Delta}{\alpha\sqrt{K}}\right)\right]/\sinh\left(\frac{\Delta}{\alpha\sqrt{K}}\right) \tag{19}$$

$$F_1 = \frac{1}{(H-\Delta)\left[\frac{\alpha}{\sqrt{K}}\coth\left(\frac{\Delta}{\alpha\sqrt{K}}\right) - \frac{\beta}{\sqrt{K}} + \frac{1}{H-\Delta}\right]} \tag{20}$$

$$\begin{aligned}F_2 = {} & \frac{\frac{\alpha}{\sqrt{K}}\left[\coth\left(\frac{\Delta}{\alpha\sqrt{K}}\right) - \operatorname{csch}\left(\frac{\Delta}{\alpha\sqrt{K}}\right)\right] + \frac{H-\Delta}{2}}{\frac{\alpha}{\sqrt{K}}\coth\left(\frac{\Delta}{\alpha\sqrt{K}}\right) - \frac{\beta}{\sqrt{K}} + \frac{1}{H-\Delta}} \\ & + \frac{\bar{\ell}\left[\operatorname{csch}\left(\frac{H-\Delta}{\bar{\ell}}\right) - \coth\left(\frac{H-\Delta}{\bar{\ell}}\right)\right]}{\frac{\alpha}{\sqrt{K}}\coth\left(\frac{\Delta}{\alpha\sqrt{K}}\right) - \frac{\beta}{\sqrt{K}} + \frac{1}{H-\Delta}}\end{aligned} \tag{21}$$

where $\alpha = (\mu^*/\mu)^{1/2}$, $\bar{\ell} = (\eta/\mu)^{1/2}/c$, $K = k/c^2$, $\Delta = \delta/c$, $H = h/c$, $Y = y/c$, $P = pc^2/\mu UR$, $\bar{u}^* = u^*/U$, $\bar{w}^* = w^*/U$, $\bar{u} = u/U$, $\bar{w} = w/U$.

The couple stress parameter $\bar{\ell}$ arises from the presence of polar additives in the lubricant. The dimension of the ratio (η/μ) is of length square and this length is of the same order of magnitude as the chain length of the polar additives in the lubricant. Hence, the couple stress parameter $\bar{\ell}$ provides the mechanism of interaction of the fluid with the bearing geometry. The additives effects are more prominent when either the chain length of the polar additives is large or the minimum film thickness is small, i.e. when $\bar{\ell}$ is large.

Substituting equations (15)–(18) into the continuity equation (Equation (6)) and integrating across the film thickness using the boundary conditions (10) and (14), the modified Reynolds equation can be written in the following dimensionless form

$$\frac{\partial}{\partial\theta}\left[G\frac{\partial P}{\partial\theta}\right] + \left(\frac{R}{L}\right)^2\frac{\partial}{\partial Z}\left[G\frac{\partial P}{\partial Z}\right] = 6\frac{\partial B}{\partial\theta} \tag{22}$$

where

$$\begin{aligned}G = {} & 12F_2H^* + 12K(\Delta - 2H^*) + 6(H-\Delta)F_2 \\ & + (H-\Delta)^3 - 12\bar{l}^2(H-\Delta) \\ & + 24\bar{l}^3\left[\coth\left(\frac{H-\Delta}{\bar{l}}\right) - \operatorname{csch}\left(\frac{H-\Delta}{\bar{l}}\right)\right]\end{aligned} \tag{23}$$

$$B = (H-\Delta)(F_1+1) + 2F_1H^* \tag{24}$$

$$H^* = \alpha\sqrt{K}\left[\coth\left(\frac{\Delta}{\alpha\sqrt{K}}\right) - \operatorname{csch}\left(\frac{\Delta}{\alpha\sqrt{K}}\right)\right] \tag{25}$$

$$H = 1 + \varepsilon\cos(\theta - \Phi) + C_0P \tag{26}$$

where $\theta = x/R$, $Z = z/L$, $\varepsilon = e/c$, $C_0 = \frac{(1+v)(1-2v)}{1-v}\left(\frac{\mu U}{ER}\right)\left(\frac{t_\ell}{R}\right)\left(\frac{c}{R}\right)^{-3}$.

The flexibility parameter C_0 is obtained from the thin liner model [16–19].

The following boundary conditions for the oil pressure in the fluid film region are adopted according to the geometric configuration, the feeding condition, and periodic condition: $P = P_s$ at oil supply groove, $P = 0$ at axial ends, and $P(\theta, Z) = P(\theta + 2\pi, Z)$. The iterative numerical scheme presented in Elsharkawy [20] is used to solve the mathematical model, which consists of the modified Reynolds equation and the film thickness equation. In this scheme, Elrod's [21] cavitation algorithm, which satisfied the conservation of mass flow across the rupture and reformation boundaries, was implemented in the numerical scheme to predict the cavitation boundary more accurately than the conventional analysis, which uses the Reynolds condition. The pressure distribution, the film shape within the lubricant film region, and the attitude angle are the outputs of the numerical solution. Then the

performance parameters such as the load carrying capacity, side leakage flow, and friction factor can be calculated.

The resultant dimensionless load carrying capacity W can be determined as follows

$$W = \frac{w_{\text{load}} c^2}{\mu U R^2 L} = \left(W_1^2 + W_2^2\right)^{1/2} \tag{27}$$

where

$$W_1 = -\int_0^1 \int_0^{2\pi} P(\theta, Z) \cos\theta \, \mathrm{d}\theta \, \mathrm{d}Z \tag{28}$$

$$W_2 = \int_0^1 \int_0^{2\pi} P(\theta, Z) \sin\theta \, \mathrm{d}\theta \, \mathrm{d}Z \tag{29}$$

where W_1 and W_2 are the dimensionless film force components along and perpendicular to the line of centers, respectively.

The friction factor and side leakage flow can be determined as

$$f\frac{R}{c} = \frac{1}{W}\int_0^1 \int_0^{2\pi} \left.\frac{\partial \bar{u}}{\partial Y}\right|_{Y=H} \mathrm{d}\theta \, \mathrm{d}Z \tag{30}$$

$$Q_s = \frac{q_s}{URc} = -2\int_0^{2\pi} \int_0^{H} \bar{w}|_{Z=0} \, \mathrm{d}Y \, \mathrm{d}\theta \tag{31}$$

4. Results and discussion

The present analysis showed that the non-Newtonian behavior of the lubricant can be described by five parameters in addition to the lubricant viscosity μ. These parameters are: couple stress parameter $\bar{\ell}$, dimensionless porous layer thickness Δ, stress jump parameter β, viscosity ratio parameter α, and permeability parameter K. These parameters describe the experimentally observed features of the behavior of the lubricant during operation. Also these parameters can be estimated experimentally. For example as mentioned by Tichy [11], the viscosity of the lubricant and the porosity of the porous layer can be measured in viscometric experiments, including the drainage experiment of Chan and Horn [10]. The thickness of the porous layer presumably can be found knowing the lubricating material's molecular structure. Ocha-Tapia and Whitkar [14] described how the stress jump could be estimated. Stokes [22] presented how the couple stress parameter can be obtained experimentally. The couple stress parameter can be also predicted from the pressure measurements using the inverse approach proposed by Elsharkawy and Guedouar (2001). The design parameters that describe the bearing configuration are the eccentricity ratio ε, journal length-to-diameter ratio L/D, and flexibility parameter C_0. A computer program was developed to investigate the effects of the lubricant parameters on the performance of hydrodynamically lubricated finite journal bearings. The numbers of the grid points in the circumferential and axial directions are 181 and 81, respectively.

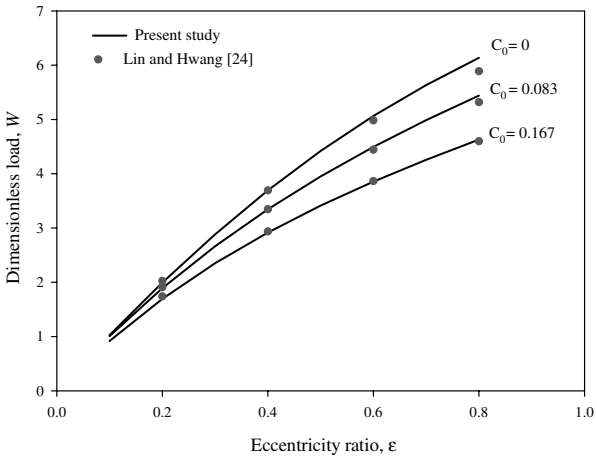

Figure 2. Comparison with the results by Lin and Hwang [24] when $L/D \to \infty$ (long bearing), $t_\ell/c = 200$, $\bar{\ell} = 0$, $\beta = 0$, $K = 2.0833 \times 10^{-4}$, and $\alpha = 1$.

To establish the validity of the solution algorithm and the computer code employed in the present study, comparisons between the results of the present numerical solution and the available theoretical results from previous studies were conducted. For the purpose of comparison, the thickness of the boundary layer is set to zero and the elastic liner is considered as a porous matrix since previous studies are special case of the present analysis. Figure 2 shows good agreement between the results obtained from the present analysis and that of Lin and Hwang [24] in the case of long journal bearing with a porous liner. Furthermore, good agreement with Chen *et al.* [25] results in the case of finite journal bearing with a porous liner as shown in figure 3.

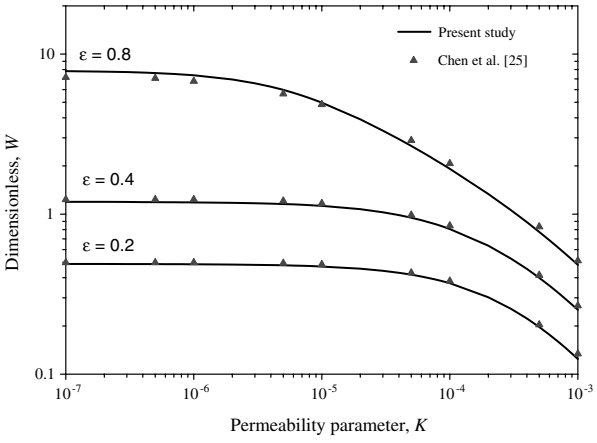

Figure 3. Comparison with the results by Chen *et al.* [25] when $L/D = 1$, $t_l/c = 200$ $\bar{\ell} = 0$, $C_0 = 0$, $\beta = 0$, and $\alpha = 1$.

Table 1.
Effects of operating parameters on steady-state performance characteristics for 12 different cases.

	Design parameters			Non-Newtonian parameters					Performance parameters				
Case	ε	L/D	C_0	$\bar{\ell}$	Δ	K	α	β	P_{max}	Φ	W	fR/c	Q_s
1	0.5	1	0	0	0	0	1	0	1.8832	60.3	1.6458	4.6233	0.7785
2	0.5	1	0	0.1	0.01	0.001	1.2	0.5	2.3861	56.9	2.0261	3.8012	0.7888
3	0.5	1	0	0.1	0.02	0.001	1.2	0.5	2.4301	56.7	2.0594	3.7508	0.7895
4	0.5	1	0	0.1	0.05	0.001	1.2	0.5	2.6187	55.7	2.2038	3.5635	0.7921
5	0.5	1	0	0.1	0.1	0.001	1.2	0.5	3.3215	52.6	2.7412	3.0601	0.7993
6	0.5	1	0	0.1	0.2	0.001	1.2	0.5	6.3709	42.4	5.0509	1.9907	0.8046
7	0.5	1	0	0.2	0.05	0.001	1.2	0.5	4.3053	48.5	3.4643	2.3007	0.8038
8	0.5	1	0	0.2	0.2	0.001	1.2	0.5	10.6301	32.8	8.5986	1.1746	0.7772
9	0.5	1	0.01	0.2	0.2	0.001	1.2	0.5	7.5483	31.4	7.1061	1.3419	0.7542
10	0.5	1	0.01	0.2	0.2	0.001	1.2	0.8	6.8855	33.4	6.3730	1.4243	0.7681
11	0.5	1	0.02	0.2	0.2	0.001	1.2	0.8	5.6528	33.1	5.5957	1.5695	0.7430
12	0.5	1	0.02	0.2	0.2	0.01	1.2	0.8	3.7576	42.1	3.5247	2.1298	0.7628

Table 1 shows the effects of different operating parameters on the steady state performance of a journal bearing for 12 different cases. The effect of the thickness of the porous layer Δ on the performance characteristics can be observed from cases 1 to 6. By increasing the thickness of the porous layer Δ, both the maximum pressure and the load carrying capacity increase, and the friction factor decreases. The significant effect of the flexibility parameter C_0 can be noticed by comparing case 8 with case 9 and case 10 with case 11. The flexibility of the liner reduces the load carrying capacity and increases the friction factor. Comparing case 4 with case 7 shows that increasing the couple stress parameter will enhance the load carrying capacity and reduce the friction factor. The dimensionless pressure distribution and the dimensionless circumferential interfacial velocity at the porous layer/fluid film interface (i.e. $Y = \Delta$) for case 12 are displayed in figures 4 and 5, respectively. The dimensionless circumferential velocity profiles at $\theta = 234^\circ$ and $Z = 0.5$ for cases 1, 3, 5, and 6 are shown in figure 6. The velocity profile for Newtonian case is also shown. It is observed that as the porous layer thickness increases the resistance to the flow within the porous media increases. Therefore, it is expected that the film pressure will increase as Δ increases.

Figure 7 illustrates the effects of stress jump parameter β on the circumferential velocity profiles at $\theta = 234^\circ$ and $Z = 0.5$ when $\varepsilon = 0.5$, $L/D = 1$, $C_0 = 0$, $\bar{\ell} = 0.2$, $\Delta = 0.2$, $K = 0.001$, and $\alpha = 1.2$. As β increases, the circumferential flow increases. It is expected that this excess flow will decrease the pressure

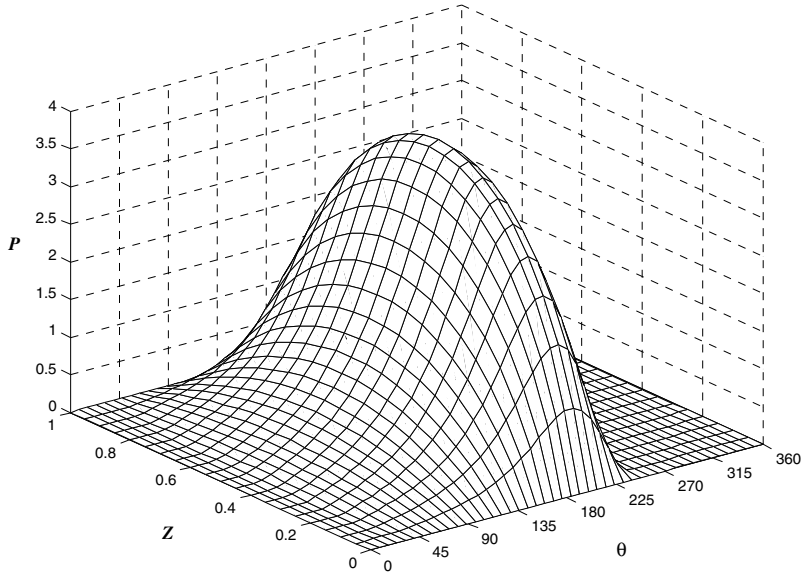

Figure 4. Pressure distribution $\varepsilon = 0.5$, $L/D = 1$, $C_0 = 0.02$, $\bar{\ell} = 0.2$, $\Delta = 0.2$, $\beta = 0.8$, $K = 0.01$, and $\alpha = 1.2$.

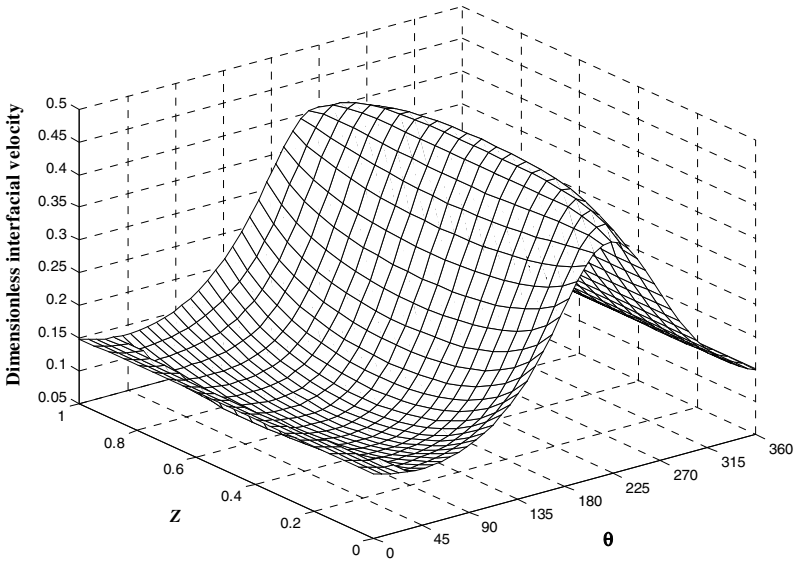

Figure 5. Dimensionless circumferential interfacial velocity distribution at the porous layer/fluid film interface when $\varepsilon = 0.5$, $L/D = 1$, $C_0 = 0.02$, $\bar{\ell} = 0.2$, $\Delta = 0.2$, $\beta = 0.8$, $K = 0.01$, and $\alpha = 1.2$.

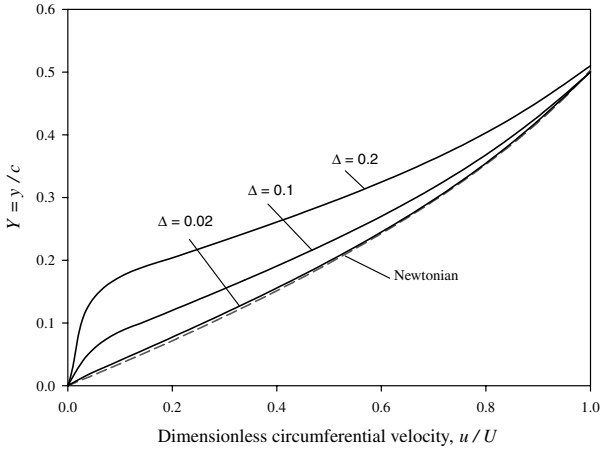

Figure 6. Effect of porous layer thickness on circumferential interfacial velocity profiles when $\varepsilon = 0.5$, $L/D = 1$, $C_0 = 0.2$, $\bar{\ell} = 0.2$, $\beta = 0.5$, $K = 0.001$, and $\alpha = 1.2$.

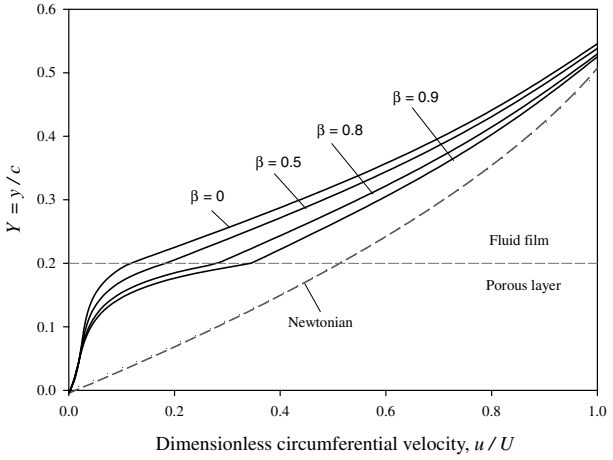

Figure 7. Effect of stress jump parameter on circumferential interfacial velocity profiles when $\varepsilon = 0.5$, $L/D = 1$, $C_0 = 0$, $\bar{\ell} = 0.2$, $\Delta = 0.2$, $K = 0.001$, and $\alpha = 1.2$.

generation within the lubricated conjunction, and as a result the load carrying capacity will decrease. It can be concluded that the stress jump parameter β has significant influence on the circumferential velocity profile and consequently will affect the lubrication performance of the bearing.

The variations of the dimensionless load carrying capacity W, and friction factor fR/c with the eccentricity ratio ε are displayed in figure 8 for different values of the couple stress parameter $\bar{\ell}$. The other parameters were held fixed at $L/D = 1$, $C_0 = 0$, $\Delta = 0.1$, $\beta = 0.5$, $K = 0.001$, and $\alpha = 1.2$. The Newtonian case is also shown. For a given value of the couple stress parameter $\bar{\ell}$, as the eccentricity ratio ε increases, the load carrying capacity increases and the friction factor decreases. In all cases, the Newtonian model gives the lowest W and the highest fR/c. The higher the eccentricity ratio the more pronounced is the effect of $\bar{\ell}$. From the definition of the couple stress parameter $\bar{\ell}$, it can be concluded that additives with larger chain length molecules can enhance the load carrying capacity and reduce the friction in journal bearings.

Figure 9 shows the variations of the dimensionless load carrying capacity W, the friction factor fR/c, and the side leakage flow Q_s with the permeability parameter of the porous layer K for different values of the dimensionless thickness of the porous layer Δ and two values of the stress jump parameter β. The other parameters were held fixed at $\varepsilon = 0.5$, $L/D = 1$, $C_0 = 0$, $\bar{\ell} = 0.2$, and $\alpha = 1.2$. Solid curves in the figures correspond to $\beta = 0.5$ and dashed curves to $\beta = 0.8$. The results show that as the thickness of the porous layer increases, the load carrying capacity increases, the coefficient of friction decreases, and the side leakage decreases. Significant reduction in the side leakage

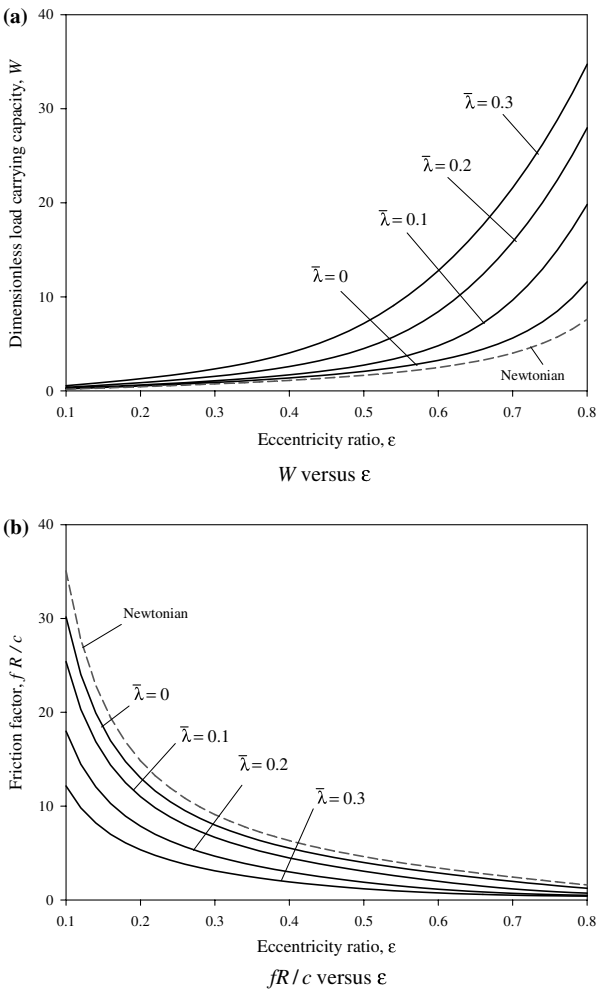

Figure 8. Variations of dimensionless load carrying capacity W, and friction factor fR/c with eccentricity ratio ε for various values of couple stress parameter $\bar{\ell}$ when $L/D = 1$, $C_0 = 0$, $\Delta = 0.1$, $\beta = 0.5$, $K = 0.001$, and $\alpha = 1.2$.

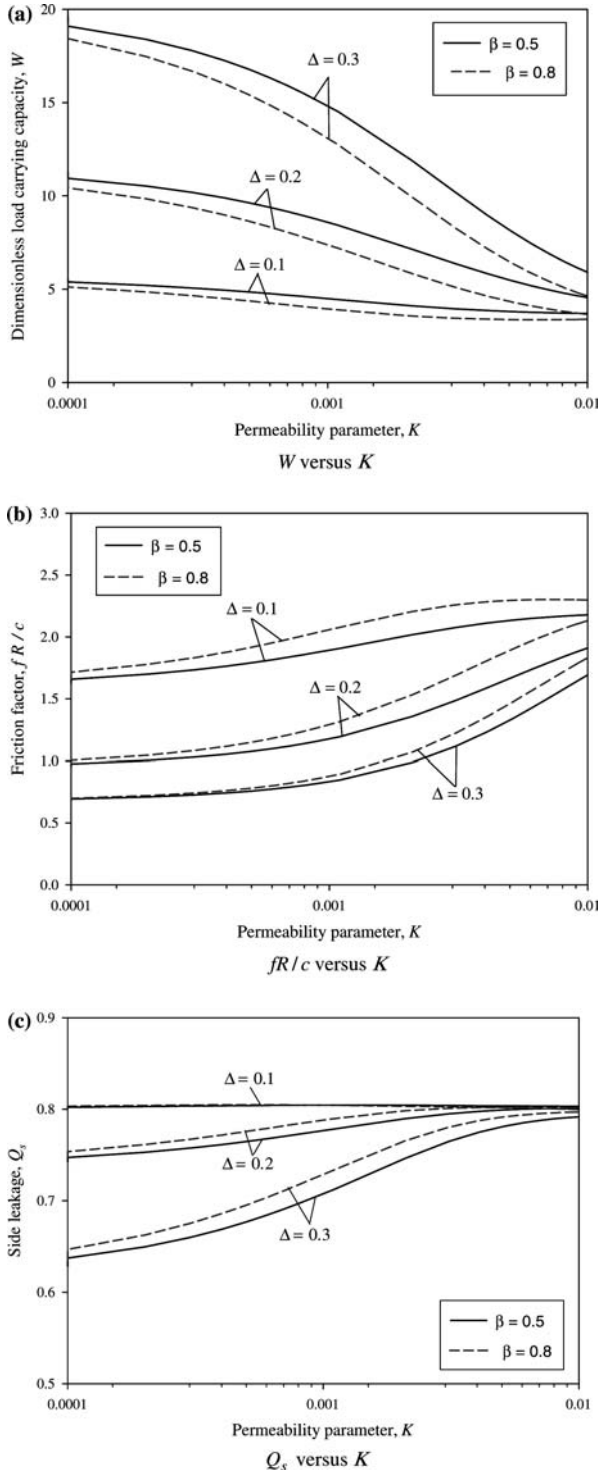

Figure 9. Variations of dimensionless load carrying capacity W, friction factor fR/c, and side leakage Q_s with permeability parameter K for various values of dimensionless porous layer thickness Δ and two values of stress jump parameter β when $\varepsilon = 0.5$, $L/D = 1$, $C_0 = 0$, $\bar{\ell} = 0.2$, and $\alpha = 1.2$.

flow can be noticed in the case of thicker porous layer ($\Delta = 0.3$). On the other hand, as the permeability parameter increases, the load carrying capacity decreases, and both the friction factor and side leakage flow increase. This is because the flow resistance in the porous region decreases as the permeability increases. The effect of the porous layer can be neglected when $K > 0.01$ regardless of the porous layer thickness. Tichy [11] and Li [12] reported similar results in the case of slider bearing. It can be seen from the results presented in figure 9 that the load carrying capacity for $\beta = 0.5$ is higher than that for $\beta = 0.8$. The increase in the stress jump parameter provides a decrease in the load capacity and an increase in both the coefficient of friction and side leakage flow. It can be concluded that additives that increase the lubricant ability to adhere to the bearing surface and form a thin solid layer will significantly enhance the load carrying capacity and reduce the friction coefficient.

The variations of the dimensionless load carrying capacity W, friction factor fR/c, dimensionless side leakage Q_s, and attitude angle Φ with the stress jump

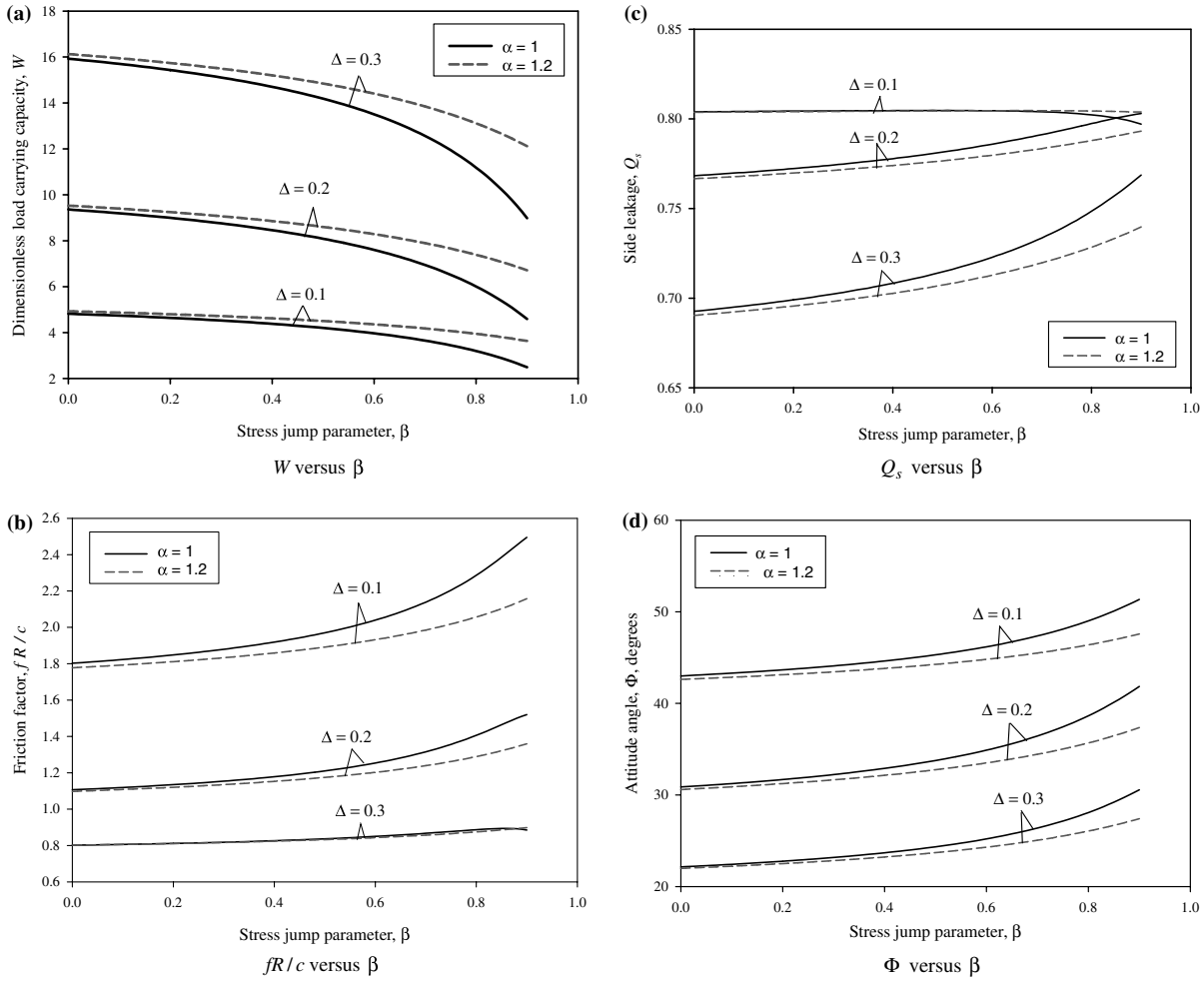

Figure 10. Variations of dimensionless load carrying capacity W, friction factor fR/c, side leakage Q_s, and attitude angle Φ with stress jump parameter β for various values of dimensionless porous layer thickness Δ and two values of viscosity ratio α when $\varepsilon = 0.5$, $L/D = 1$, $C_0 = 0$, $\bar{\ell} = 0.2$, and $K = 0.001$.

parameter β are depicted in figure 10 for different values of the dimensionless thickness of the porous layer Δ and two values of the viscosity ratio α. The other parameters were held fixed at $\varepsilon = 0.5$, $L/D = 1$, $C_0 = 0$, $\bar{\ell} = 0.2$, and $K = 0.001$. Solid curves in the figures correspond to $\alpha = 1$ and dashed curves to $\alpha = 1.2$. The influence of the stress jump parameter is more pronounced when $\beta > 0.5$. The viscosity ratio parameter α indicates the value of the lubricant viscosity within the boundary layer μ^* relative to the viscosity within the fluid film μ (i.e. $\alpha = 1$ means $\mu^* = \mu$ and $\alpha = 1.2$ means $\mu^* = 1.44\mu$). Physically, it is expected that the viscosity of the lubricant within the porous layer will be higher than the viscosity of the lubricant within the fluid film (i.e. $\alpha > 1$). As the viscosity of the lubricant within the porous layer increases, the flow resistance will increase resulting in an increase in the fluid film pressure. The performance of the journal bearing can be also improved as the viscosity ratio increases. It is alo found that the attitude angle Φ decreases as the porous layer thickness increases, and it increases slightly as the stress jump parameter β increases.

Variations of dimensionless load carrying capacity W^*, friction factor fR/c, side leakage flow Q_s, and attitude angle Φ with length-to-diameter ratio L/D are shown in figure 11 for various values of the dimensionless porous layer thickness Δ. The other parameters were held fixed at $\varepsilon = 0.5$, $C_0 = 0$, $\bar{\ell} = 0.2$, $\beta = 0.5$, $K = 0.001$, and $\alpha = 1.2$. For a given value of Δ, the load carrying capacity and the side leakage flow increase as the length-to-diameter ratio L/D increases. On the other hand, the friction factor fR/c decreases as L/D increases. The effect of the porous layer thickness on the side leakage flow is more pronounced when $L/D > 1$ (i.e. long bearing). The results presented in figure 11 confirm the significant effect of the thickness of the porous layer on the performance of journal bearings for wide range of L/D ratio.

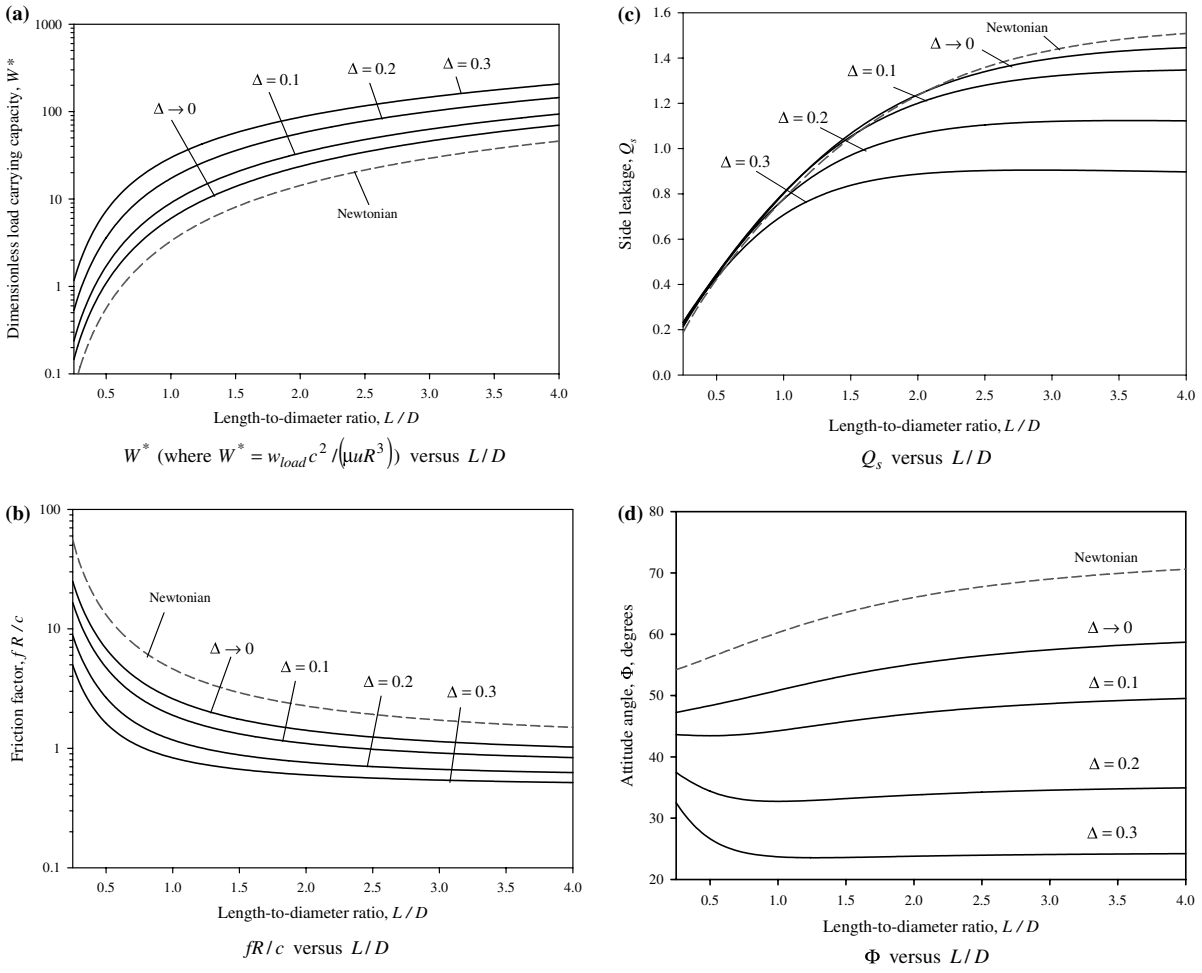

Figure 11. Variations of dimensionless load carrying capacity W^*, friction actor fR/c, side leakage Q_s, and attitude angle Φ with length-to-diameter ratio L/D for various values of dimensionless porous layer thickness Δ when $\varepsilon = 0.5$, $C_0 = 0$, $\bar{\ell} = 0.2$, $\beta = 0.5$, $K = 0.001$, and $\alpha = 1.2$.

5. Conclusions

A non-Newtonian rheological model to investigate theoretically the effects of the lubricant additives on the hydrodynamic lubrication of journal bearings has been presented. The proposed model combines the thin porous media model, which was developed by Tichy [11] and refined by Li [12] to simulate the microstructure of the lubricant, and the couple stress model to incorporate the effects of polar additives in the lubricant. A modified form of Reynolds equation has been derived and solved numerically using a finite difference scheme. The present analysis exhibits additive effects through five parameters. These parameters are: couple stress parameter $\bar{\ell}$, dimensionless porous layer thickness Δ, stress jump parameter β, viscosity ratio parameter α, and permeability parameter K. The results showed that additives that increase the lubricant ability to form a thin solid layer that adheres to the bearing surface could significantly enhance the load carrying capacity and reduce the friction coefficient. Furthermore, additives with larger chain length molecules can also enhance the load carrying capacity and reduce the coefficient of friction.

Acknowledgments

This work was done while on sabbatical leave during academic year 2003–2004 at Northwestern University, USA, and Cardiff University, UK. The sabbatical leave support of Kuwait University and the hospitality of Northwestern University and Cardiff University are much appreciated.

References

[1] D.R. Oliver, J. Non-Newtonian Mech. 31 (1988) 185.
[2] A.H. Spikes, J. Proc. Ins. Mech. Eng. 28 (1994) 3.
[3] E. Durak, C. Kurbanoglu, A. Biyiklioglu and H. Kaleli, Tribol. Int. 36 (2003) 599.
[4] I.K. Dien and H.G. Elrod, ASME, J. Lubr. Technol. 105 (1983) 385.
[5] W.L. Li, C.I. Weng and J.I. Lue, STLE, Tribol. Trans. 39(4) (1996) 819.
[6] V.K. Stokes, Phys. Fluids 9 (1966) 1709.
[7] R.S. Gupta and L.G. Sharma, Wear 125 (1988) 257.

[8] J.R. Lin, C.B. Yang and R.F. Lu, Tribol. Int. 34 (2001) 119.
[9] X.L. Wang, K.Q. Zhu and S.Z. Wen, Tribol. Int. 35 (2002) 185.
[10] D.Y.C. Chan and R.G. Horn, J. Chem. Phys. 83(10) (1985) 5311.
[11] J.A. Tichy, Trans. ASME, J. Tribol. 117 (1995) 16.
[12] W.L. Li, Trans. ASME, J. Tribol. 121 (1999) 823.
[13] D.A. Nield, Int. J. Heat Fluid Flow 12 (1991) 269.
[14] J.A. Ochoa-Tapia and J. Whitaker, Int. J. Heat Mass Transfer 38 (1995) 2635.
[15] H.C. Brinkman, Appl. Sci. Res. A1 (1984) 27.
[16] G.R. Higginson, Proc. Symp. On Elastohydrodynamic Lubrication, Instn. Mech. Engrs., 180(Part 3B) (1965) 31.
[17] J. O'Donoghue, D.K. Brighton and C.J.K. Hooke, Trans. ASME, J. Lubr. Technolo. 89(4, Series F) (1967) 409.
[18] H.D. Conway and H.C. Lee, Trans. ASME, J. Lubr. Technol. 97 (1975) 599.
[19] M. Lahmar, A. Haddad and D. Nicolas, J. Eng. Tribol. Proc. Inst. Mech. Eng. 212(Part J) (1988) 193.
[20] A.A. Elsharkawy, STLE, Tribol. Trans. 46(1) (2003) 119.
[21] H.G. Elrod, Trans. ASME, J. Lubr. Technol. 103 (1981) 350.
[22] V.K. Stokes, *Theories of Fluids with Microstructure—An Introduction* (Springer-Verlag, Berlin, Heidelberg, New York, Tokyo 1984).
[23] A.A. Elsharkawy and L.H. Guedouar, Tribol. Int. 34 (2001) 107.
[24] J.R. Lin and C.C. Hwang, Wear 161 (1996) 93.
[25] M.D. Chen, K.M. Chang, J.W. Lin and W.L. Li, Tribol. Int. 35 (2002) 287.